Integration of Antenna Array and Self-Switching Graphene Diode for Detection at 28 GHz

Integration of antenna array and self-switching graphene diode for detection at 28 GHz

M. Yasir, Student *Member*, *IEEE*, M. Aldrigo, M. Dragoman, A. Dinescu, M. Bozzi, *Fellow*, *IEEE*, S. Iordanescu, *Member*, *IEEE*, D. Vasilache

***Abstract*—In this paper, a rectenna based on a graphene self-switching diode is presented. The nonlinear behavior of the diode is beneficial to efficiently detect the RF power in the Ka band. The target operating frequency of 28 GHz is of particular interest for the upcoming 5G and internet-of-things telecommunication systems in the range 1–100 GHz. The 4-element patch antenna array was designed for an on-wafer high-resistivity silicon/silicon dioxide/graphene multi-layer system. Then, the optimal number of parallel channels for the diode was calculated by using analytical formulas, in order to achieve the highest possible DC current and nonlinearity. Finally, the diode was integrated in a coplanar waveguide structure with open stub, in order to maximize the array-to-diode power transfer. This step-by-step optimization resulted in a high yield rate, a DC current of over ±1.2 mA at ±3 V, a responsivity of 96 V/W at 28 GHz and a NEP of 692 pW/√Hz, with maximum measured values of 95 mV for the DC voltage and of almost 4.5 μW for the DC power, for an RF input power of about 500 μW.**

***Index Terms*—Antenna arrays, graphene, diodes, signal detection.**

I. Introduction

Detection of low-power signals is a very important issue for radar applications at microwaves [1], as well as for the next-generation of 5G communications and internet-of-things (IoT) in the range 1–100 GHz. Some bands are of great importance, such as 28 GHz (permitted for 5G use) and 60 GHz for high-rate wireless systems [2]. The development of IoT is tightly bound to self-powering devices [3-5]. For this purpose, electromagnetic (EM) detection in the super high frequency band (SHF, 3–30 GHz) is a crucial research area, which relies upon efficient antenna geometries integrated with a rectifying diode ("rectennas" [6]). Classic Schottky diodes make use of novel materials (like diamond and graphene [7,8]). In this respect, a promising technology is represented by the self-switching diodes (SSD), i.e. planar semiconductor/semimetal diodes, used especially for THz applications [9]. Their working principle is based on a nonlinear current flow through nanometer-sized parallel channels, controlled by field-effect phenomena. The SSD is a geometrical diode: no junctions are necessary, hence no doping (which has detrimental effects in case of graphene monolayers). The geometrical design parameters of the SSD are of utmost importance for the optimization of its performance. In detail, the width of the channel is given by lithographic constraints, whereas the channel length and the number of channels are the main targets of the design optimization process. Up to now, SSD detectors have successfully been realized deploying various materials, such as graphene for microwave and millimeter waves [10,11], reduced graphene oxide/ZnO, InP/InGaAs/InP, AlGaN/GaN and InAs [12–15], and the most promising results have been obtained with GaAs SSDs (NEP of 330 pW/√Hz at 1.5 THz). Nevertheless, to the authors' knowledge, no attempt has been made to fully integrate an SSD with an antenna radiating system, so as to create an SSD-based rectenna and to demonstrate its effective microwave detection capabilities. In this paper, we aim at filling this gap by presenting the fabrication and experimental characterization of a graphene SSD (GSSD) integrated with a patch antenna array, for EM detection at 28 GHz. Wafer-level fabrication on 4-inch Si/SiO_2 wafer covered with graphene monolayer, high fabrication yield and very high DC current of the GSSDs represent the major results of the proposed research.

The Romanian authors thank the financial support from the Romanian Ministry of Research and Innovation, via the project NUCLEU 2018 MICRO-NANO-SIS, contract no. 4N/2018, via the project M-TMA-ID (PN-III-P1-1.1-PD-2016-0535), contract no. 58/2018, and via the project GRAPHENEFERRO, contract no. PN-III-P4-ID-PCCF-2016-0033.

M. Yasir and M. Bozzi are with the Microwave Lab, Dept. of Electrical Computer and Biomedical Engineering, University of Pavia, Pavia, 27100 Italy (e-mail: muhammad.yasir01@universitadipavia.it, maurizio.bozzi@unipv.it).

M. Aldrigo, M. Dragoman, A. Dinescu, S. Iordanescu and D. Vasilache and are with the National Institute for Research and Development in Microtechnologies (IMT), 077190 Voluntari (Ilfov), Romania (e-mail: {martino.aldrigo; mircea.dragoman; adrian.dinescu; sergiu.iordanescu; dan.vasilache}@imt.ro).

II. Graphene Self-Switching Diode: Modeling, Fabrication and Performance

Since an SSD is a two-terminal geometrical diode, the fabrication is performed with minimal process steps. An SSD can be modeled very simply as a two-dimensional field-effect transistor (FET), with short-circuited gate and drain, made of narrow channels in parallel [16]. Its nonlinear I-V behavior can be used for detection of radio frequency signals. First, we investigated the geometric layout of the GSSD able to guarantee the highest nonlinearity and DC current (I_d) values. The GSSD can be modeled as a capacitive divider with quantum capacitance C_q and substrate capacitance C_s in series. Each channel couples capacitively to the applied drain bias

voltage (V_d) via C_q and C_s. The modeling procedure is presented in [11] and we have $I_d \approx N\mu_{eff}C_s\frac{w}{\ell}|V_d - V_D|V_d$, where N is the number of channels, μ_{eff} is the effective channel (graphene) mobility, w is the distance between adjacent channels, ℓ is the length of the channel and V_D is the Dirac voltage (set equal to zero). After an optimization process on I_d to maximize the performance at low values of the DC bias, we obtained N=12, w_0=w=100 nm and ℓ=1.1 μm. This means that the whole GSSD is made of 12 channels in parallel, which entails that the currents flowing along each channel sum up, thus increasing the total current of the device and reducing the total parallel resistance. The reference substrate is a 4-inch high-resistivity silicon/silicon dioxide (HRSi/SiO_2) wafer, with thickness of 525 μm/300 nm (respectively); the HRSi has a nominal resistivity of 10,000 Ω·cm. To properly measure the GSSDs in DC and at microwaves, we resumed to a coplanar waveguide (CPW) structure with open stubs of different lengths (namely 300, 500, 700 and 900 μm), in order to provide different reactance values suitable to optimize the impedance matching to 50 Ω in correspondence of the port connected to the antenna array. This guarantees the maximum power transfer from the array to the diode that detects/rectifies the RF signal. As regards the fabrication of the GSSDs, first the CVD-grown graphene monolayer (by Graphenea) was fixed in the diodes' location using two rectangular metal pads. The diodes were patterned by e-beam lithography using PMMA 950k as electronresist and O_2 plasma etching. To remove the graphene from the wafer surface, the diodes were covered by a negative electronresist –hydrogen silsesquioxane (HSQ)– patterned by e-beam lithography, defining rectangular protective areas on top of diodes and the residual graphene was etched away in oxygen plasma. The fabricated devices are shown in Fig. 1: Fig. 1a is an optical picture of the CPW-based devices with stubs of different lengths (denoted by the numbers under each device), the inset being a magnification of the diode area with the HSQ thin film on the graphene monolayer; Fig. 1b is a SEM picture of the GSSD with four channels. Fig. 2 shows the measured I-V characteristic of a fabricated GSSD. All measurements were carried out at room temperature (T=290 K) using a Keithley SCS 4200 station. The maximum DC current value is over ±1.2 mA at ±3 V (a major results w.r.t. state-of-the-art GSSDs) thanks to the optimized nanolithography process for multiple channels in parallel. We also extracted the values of frequency-dependent equivalent resistance (R_{eq}) and capacitance (C_{eq}) of the diode (calculated from an equivalent R-C parallel circuit, seen from the port directly connected to the GSSD): in this case, in the band of interest (i.e. 26–30 GHz) the average value of the resistance is around 264 Ω (it can be considered, with good approximation, the combination of the total parasitic linear resistance $R_{s,tot}$ and of the intrinsic nonlinear resistance R_i that represents the electrical nonlinearity of the GSSD [17]), whereas the average value for the capacitance is around 68.36 fF. The differential resistance of the diode R_D (defined as R_D=$\partial V_d/\partial I_d$) spans the range 1.5–5 kΩ. The yield rate of the fabrication is very high: over 90% of the fabricated devices show the same I-V characteristic. We verified that the GSSDs burn out between ±6 V and ±7 V of applied DC bias: for this reason, we did not exceed to bias the diodes over ±3 V, to

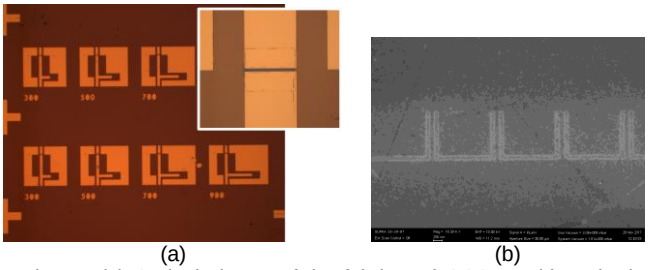

Fig. 1. (a) Optical picture of the fabricated GSSDs with stubs in CPW (inset: diode's area with HSQ thin film on graphene monolayer); (b) SEM picture of a GSSD with four channels.

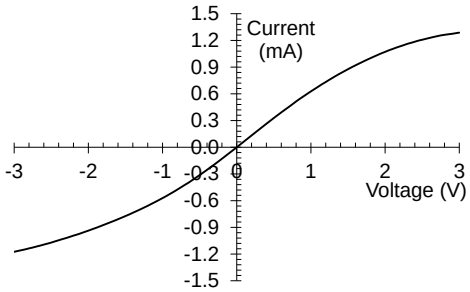

Fig. 2. Measured I-V characteristic of the generic GSSD.

avoid the saturation of the I-V characteristic. Since graphene monolayer is a semimetal exhibiting ambipolar transport, from the measured I-V curve it results that the GSSD works for both positive and negative values of the DC bias. This was reported previously [10] and can be interpreted by considering two main interacting phenomena, i.e. the charge neutrality near zero bias ($V_d \approx V_D$) and the current saturation at high bias values. At zero bias, the measured voltage responsivity at 28 GHz (when the GSSD is fed from a 50 Ω impedance with an input power of 1.22 mW) is $\beta_{50\Omega}$=7.04 V/W. The noise equivalent power at 50 Ω is $NEP_{50\Omega} = \sqrt{4K_BTR_{D0}}/\beta_{50\Omega}$ [17], where K_B is Boltzmann's constant and R_{D0}=1.48 kΩ is the zero-bias differential resistance (reduced thanks to the 12 channels in parallel). In the present case, we obtained $NEP_{50\Omega}$=691.56 pW/√Hz, which is of the same order of magnitude of the actual state-of-the-art for GSSDs [10]. Since the detection sensitivity for weak AM signals can be improved by biasing the diode (in order to move the operating point slightly closer to a higher nonlinearity, in either forward or reverse conduction), we measured the maximum value of DC bias voltage able to maximize $\beta_{50\Omega}$: it was found that the highest voltage responsivity at 28 GHz is $\beta_{50\Omega}$=96.16 V/W for a bias V_d=-1.35 V.

III. Integration of Antenna Array with GSSD

The radiating element is a 4-element patch antenna array (Fig. 3a) fabricated by means of optical lithography. The metallization is a 500 nm thick Au layer, deposited and patterned using a lift-off process. The array configuration is 2×2, the length and width of each patch antenna being L=1.5 mm (x-direction) and W=2.206 mm (y-direction), respectively, while the spacing between antennas is about $0.51\lambda_0$ in the x-direction and about $0.37\lambda_0$ in the y-direction, with λ_0≈10.71 mm the free-space wavelength at 28 GHz. These dimensions provide the optimal broadside radiation and

in-phase excitation of all the radiating elements. The reference array input impedance of 50 Ω is guaranteed by a microstrip line with a width of 300 µm. The array ensures a higher gain (i.e. about 8.1 dB from EM simulations) w.r.t. the single patch. We chose to use two arrays on the same metal support, each array connected to a GSSD with different stub length, namely 500 µm and 700 µm, in order to verify the different effect of stub's length on the array-to-diode power transfer. It was found that the antenna-GSSD matching is enhanced with the 500-µm-long stub. The array-GSSD electrical connection is performed with two 17 µm diameter Au wires (soldered in parallel, with silver conductive paste polymerized at 120 °C for 1 hour). The simulated and measured return loss ($|S_{11}|$) of the standalone array are shown in Fig. 3b. The resonance occurs at 27.8 GHz showing a very good agreement with simulation. The measured voltage standing wave ratio (VSWR) is about 1.34 and the -10 dB fractional bandwidth is 1.76%. The measurement setup for the RF characterization

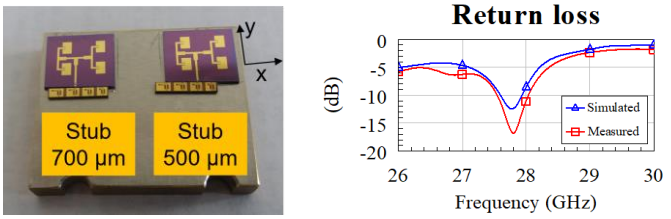

(a) (b)

Fig. 3. (a) Fabricated rectenna prototypes assembled on metal support; (b) simulated (solid blue line) and measured (solid red line) return loss of the standalone patch antenna array.

comprises an Agilent analog signal generator, connected to a horn antenna ("transmitter", Ka band, 24 dBi gain), excited by a 28 GHz sinusoidal carrier modulated by a square AM signal of frequency f_{AM}=1 kHz. The transmitter was put at various distances from the rectenna, which was connected to a Tektronix oscilloscope. The load resistance of the rectenna (connected in parallel to the oscilloscope's port) is a 2 kΩ resistor. This value of resistance was chosen as it is very close to R_D, thus enhancing the output DC signal. No optimization was carried out for the capacitive part of rectenna's load, useful to smooth out the output ripple and store the rectified energy. In order to verify the effect of a DC bias on the diode, we used a linear power supply. By varying the distance between transmitter and receiver from 5 to 15 cm (in the far field region of the rectenna), the effective RF input power delivered to the GSSD is in the range 13–470 µW. The calculated voltage responsivity $\beta_{50\Omega}$ for different values of the DC bias gives the proof that negative values provide a clear enhancement of the responsivity w.r.t. positive ones, due to diode's asymmetry, with a maximum value of 96.16 V/W at 28 GHz for V_d=-1.35 V. Considering the very low RF power levels at diode's input, the responsivity is comparable to the actual state-of-the-art for semiconductor SSDs [18,19]. Finally, in Fig. 4a the measured DC voltage V_{DC} and power P_{DC} is presented as a function of the distance between transmitter and rectenna, for V_d=-0.66 V and for two values of the power at transmitter's input (i.e. 1 mW and 0.25 mW). The maximum values are V_{DC}=94.5 mV and P_{DC}=4.47 µW at 5 cm distance, whereas the minimum values are V_{DC}=3.8 mV and P_{DC}=7 nW at 15 cm distance. Beyond V_d=-0.66 V, the performance of the GSSD does not change due to saturation of the I-V characteristic. Moreover, higher values of RF input power seem to affect graphene's atomic structure, causing a degradation of diode's performance (and a decrease of V_{DC}). A further proof of the detection capabilities of the proposed rectenna is given in Fig. 4b, which is a screenshot of the detected voltage: the AM signal is well shaped in all the measured situations.

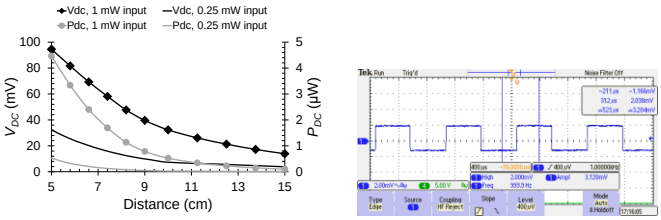

(a) (b)

Fig. 4. (a) Measured DC voltage (left axis, black lines) and power (right axis, grey lines); (b) screenshot of the detected voltage.

REFERENCES

[1] S. Vishwakarma, V. Ummalaneni, M. S. Iqbal, A. Majumdar, and S. S. Ram, "Mitigation of through-wall interference in radar images using denoising autoencoders," *Proc. of 2018 IEEE Radar Conference (RadarConf18)*, pp. 1543–1548, 23-27 Apr. 2018, DOI: 10.1109/RADAR.2018.8378796

[2] S. K. Yong, and C.-C. Chong, "An overview of multigigabit wireless through millimeter wave technology: Potentials and technical challenges," *EURASIP Journal on Wireless Communications and Networking*, vol. 2007, pp. 1–10, 2007, DOI: 10.1155/2007/78907

[3] D. Bandyopadhyay, and J. Sen, "Internet of things: Applications and challenges in technology and standardization," *Wireless Pers. Commun.*, vol. 58, no. 1, pp. 49–69, 2011, DOI: 10.1007/s11277-011-0288-5

[4] O. Galinina, H. Tabassum, K. Mikhaylov, S. Andreev, E. Hossain, and Y. Koucheryavy, "On feasibility of 5G-grade dedicated RF charging technology for wireless-powered wearables," *IEEE Wireless Communications*, vol. 23, no. 2, pp. 28–37, Apr. 2016, DOI: 10.1109/MWC.2016.7462482

[5] A. Costanzo, and D. Masotti, "Energizing 5G: Near- and Far-Field Wireless Energy and Data Transfer as an Enabling Technology for the 5G IoT," *IEEE Microwave Magazine*, vol. 18, no. 3, pp. 125–136, May 2017, DOI: 10.1109/MMM.2017.2664001

[6] G. Moddel, S. Grover, Rectenna Solar Cells, Springer, New York (2013).

[7] T. Oishi, N. Kawano, and S. Masuya, "Diamond Schottky Barrier Diodes With NO2 Exposed Surface and RF-DC Conversion Toward High Power Rectenna," *IEEE Trans. Electron Dev. Lett.*, vol. 38, no. 1, pp. 87–90, Jan. 2017, DOI: 10.1109/LED.2016.2626380

[8] M. Dragoman, and M. Aldrigo, "Graphene rectenna for efficient energy harvesting at terahertz frequencies," *Appl. Phys. Lett.* 109, 113105 (2016), DOI: 10.1063/1.4962642

[9] P. Sangaré, G. Ducournau, B. Grimbert, V. Brandli, M. Faucher, C. Gaquière, A. Íñiguez-de-la-Torre, I. Íñiguez-de-la-Torre, J. F. Millithaler, J. Mateos, and T. González, "Experimental demonstration of direct terahertz detection at room temperature in AlGaN/GaN asymmetric nanochannels," *J. Appl. Phys.* 113, 034305 (2013), DOI: 10.1063/1.4775406

[10] A. Westlund, M. Winters, I. G. Ivanov, J. Hassan, P.-Å. Nilsson, E. Janzén, N. Rorsman, and J. Grahn, "Graphene self-switching diodes as zero-bias microwave detectors," *J. Appl. Phys.* 106, 093116 (2015), DOI: 10.1063/1.4914356

[11] M. Winters, M. Thorsell, W. Strupiński, and N. Rorsman, "High frequency electromagnetic detection by nonlinear conduction modulation in graphene nanowire diodes," *J. Appl. Phys.* 107, 143508 (2015), DOI: 10.1063/1.4932970

[12] S. Bhatnagar, R. Kumar, M. Sharma, and B. K. Kuanr, "Reduced graphene Oxide/ZnO nanostructures based rectifier diode," *AIP Conference Proc.* 1832, 050060 (2017), DOI: 10.1063/1.4980293

[13] C. Balocco, A. M. Song, M. Åberg, A. Forchel, T. Gonzálezl, J. Mateos, I. Maximov, M. Missous, A. A. Rezazadeh, J. Saijets, L. Samuelson, D. Wallin, K. Williams, L. Worschech, and H. Q. Xu, "Microwave Detection at 110 GHz by Nanowires with Broken Symmetry," *Nano Lett.*, vol. 5, no. 7, pp. 1423–1427, Jun. 2005, DOI: 10.1021/nl050779g

[14] P. Sangaré, G. Ducournau, B. Grimbert, V. Brandli, M. Faucher, C. Gaquière, A. Íñiguez-de-la-Torre, I. Íñiguez-de-la-Torre, J. F. Millithaler, J. Mateos, and T. González, "Experimental demonstration of direct terahertz detection at room-temperature in AlGaN/GaN asymmetric nanochannels," *J. Appl. Phys.* 113, 034305 (2013), DOI: 10.1063/1.4775406

[15] A. Westlund, P. Sangaré, G. Ducournau, P.-Å. Nilsson, C. Gaquière, L. Desplanque, X. Wallart, and J. Grahn, "Terahertz detection in zero-bias InAs self-switching diodes at room temperature," *Appl. Phys. Lett.* 103, 133504 (2013), DOI: 10.1063/1.4821949

[16] A. Westlund, P. Sangaré, G. Ducournau, I. Iñiguez-de-la-Torre, P.-Å. Nilsson, C. Gaquière, L. Desplanque, X. Wallart, "Optimization and Small-Signal Modeling of Zero-Bias InAs Self-Switching Diode Detectors," *Solid-State Electronics*, vol. 104, pp. 79–85, Feb. 2015, DOI: 10.1016/j.sse.2014.11.014

[17] A. Westlund, I. Iñiguez-de-la-Torre, P.-Å. Nilsson, T. González, J. Mateos, P. Sangaré, G. Ducournau, C. Gaquière, L. Desplanque, X. Wallart, and J. Grahn, "On the effect of δ-doping in self-switching diodes," *Appl. Phys. Lett.* 105, 093505 (2014), DOI: 10.1063/1.4894806

[18] H. Sánchez-Martín, S. Sánchez-Martín, O. García-Pérez, S. Pérez, J. Mateos, T. González, I. Íñiguez-de-la-Torre, C. Gaquière, "Microwave detection up to 43.5 GHz by GaN nanodiodes: Experimental and analytical responsivity," 2017 Spanish Conference on Electron Devices (CDE), Electronic ISBN: 978-1-5090-5072-7, 2017, DOI: 10.1109/CDE.2017.7905251

[19] H Sánchez-Martín, S Sánchez-Martín, I Íñiguez-de-la-Torre, S Pérez, J A Novoa, G Ducournau, B Grimbert, C Gaquière2, T González and J Mateos, "GaN nanodiode arrays with improved design for zero-bias sub-THz detection," *Semicond. Sci. Technol.* 33 095016, no. 9, Aug. 2018, DOI: 10.1088/1361-6641/aad766